

Pattern switching in soft cellular solids under compression

Cite this: *Soft Matter*, 2013, **9**, 4951

T. Mullin,* S. Willshaw and F. Box

It is becoming increasingly recognized that nonlinear phenomena give an opportunity to provide robust control of the properties of soft metamaterials. A class of elastic instabilities are discussed which arise when a soft cellular material is compressed. The global nature of the induced pattern switch makes it a prime candidate for controlling macroscopic photonic and auxetic properties of the material. We demonstrate the robustness of the phenomena using a range of soft materials and show how the shape of the repeat unit of the periodic pattern can be used to influence the global characteristics of the soft solid.

Received 20th November 2012

Accepted 19th March 2013

DOI: 10.1039/c3sm27677e

www.rsc.org/softmatter

1 Introduction

Low density cellular solids are common in nature with examples ranging in scale from cancellous bone with high strength-to-weight ratio¹ to the intricate structures on the wings of butterflies which give them their iridescent colours.² Man has exploited these features in the design of complex structures ranging from spacecraft to photonic crystals.³ When they are soft, cellular solids can be compressed using small strain fields and exhibit structural instabilities above a critical value of the applied strain.¹ The influence of instabilities on global material properties are important⁴ in broadening the functionality of materials in terms of their wetting and photonic properties. A specific example of this is provided by a novel instability uncovered when a two-dimensional elastomer with a square lattice of holes is compressed.⁵ The pattern switch which is involved is robust and has now been found at the nanoscale⁶ and applied to the control of photonic devices.³

The purpose of this article is to report on a number of observations at the macroscale which demonstrate that the pattern switch is a robust geometrical effect which is independent of the details of the material properties of the matrix. The central idea being advanced here is that it is the symmetry of the geometry of the cellular structure which is key to the pattern switch. Specifically, the strong coupling of the square geometry forces a simple bifurcation so that details of the material properties of the matrix are of secondary importance. The geometrical theme is explored using a range of soft materials and the review is concluded by reporting on the influence of hole shape on the pattern switch.

2 Pattern switching in soft cellular solids

The original experiments⁵ were performed using elastic specimens with circular holes which were accurately cut out of an elastomer sheet using water jets. The sample comprised a microstructure of a 10×10 square array of circular holes of 8.67 mm diameter with 9.97 mm center-to-center spacing, vertically and horizontally. The periodic lattice microstructures were cut from 9.4 mm thick sheets of the photoelastic elastomer PSM-4 using water jets and the samples were approximately 100 mm by

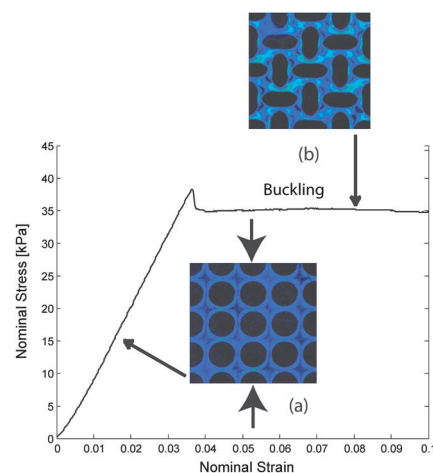


Fig. 1 Experimental results in the form of nominal stress versus nominal strain curves for a 10×10 square array of holes in a sheet of PSM-4 elastomer under compression. The dependence is approximately Hookean at small strains and all holes deform slightly as indicated in image (a) (here strain is applied uniaxially and is defined as $\epsilon = \Delta h/h$ where h is the original height of the sample and Δh is the displacement). The departure from linearity is the result of an elastic buckling instability in the microstructure that triggers a pattern transformation to an array of orthogonal ellipses (b). The material is photoelastic and concentrated regions of stress are indicated by the light colouring.

Manchester Centre for Nonlinear Dynamics, The University of Manchester, Oxford Rd, Manchester M13 9PL, UK. E-mail: tom@reynolds.ph.man.ac.uk; Fax: +44 (0)161 275 4056; Tel: +44 (0)161 275 4070

100 mm. The material has a shear modulus of 3.25 MPa and is photoelastic so that the colour variation seen in Fig. 1(b) gives an indication of the stress field. The sample was held vertically between two close fitting 5 mm thick polymethylmethacrylate (PMMA) sheets to minimise out-of-plane buckling. An Instron compression testing machine was used to apply a quasi-static uniform displacement to the sample and record its response.

The results shown in Fig. 1 provide a typical example of a stress-strain response for cellular materials¹ where stress is approximately proportional to strain for small displacements and compression within the material is taken up by fore-shortening of interstitial vertical ligaments in the structure. Above a critical values of the strain (here $\sim 4\%$), buckling of the ligaments occurs and stress becomes approximately independent of strain. The buckling is coincident with the onset of the pattern switched state shown in Fig. 1(b). The new state appears rapidly and the transition is reversible and repeatable. Its global nature is a result of the coupling of the buckling throughout the square lattice and involves the counter-rotation of neighboring interstitial four pointed star-shaped ligatures between the holes and is predicted from theory.⁷

The patterned switched state exhibits a negative value of the Poisson's ratio^{8,9} which is sometimes called 'Auxetic' behaviour. This is illustrated in the image shown in Fig. 2 where a square lattice of circular holes in a nominally two-dimensional silicone rubber elastomer has been compressed with a nominal strain of $\varepsilon = 0.25$. A clear indication of negative Poisson's ratio is that the lateral boundaries of the sample bend inwards under compression whereas a solid rubber sample will bulge. Indeed the results of a detailed numerical and experimental investigation are in good accord for this auxetic property.⁹ A limitation is that the auxetic response only occurs under compression but it is robust, it is created in a controlled way by a simple modification to the material and it will work at the nanoscale.

A moulding process was also used to create samples containing 10×10 circular holes of diameter ~ 10 mm in a set jelly. This material has Young's modulus of $\sim 10^3$ Pa (ref. 10) and deforms in plane under its own weight when held between two chalk dusted PDMS sheets as shown in Fig. 3. As can be seen, a pattern switched state where the original square array of



Fig. 2 Two dimensional silicone rubber sample under vertical compression at $\varepsilon = 0.25$. The sample was held between two loose fitting PDMS plates which prevented out of plane buckling. The sidewalls of the initial rectangular sample moved inwards under compression indicating negative Poisson ratio behaviour.



Fig. 3 Pattern switched state in a jelly which has deformed under its own weight. The initial state was a square lattice of circular holes which switched rapidly to the shown array of orthogonal ellipses when the sample was turned from lying horizontal to standing vertical.

circular holes was transformed into an array of orthogonal ellipses. The switch occurred as soon as the sample was oriented vertically.

Specific anisotropy was introduced into the jelly in a controlled yet simple manner. This is illustrated in the images shown in Fig. 4 where 8 mm long by 1 mm diameter aluminum rods were placed as shown in Fig. 4(a). They were positioned during the setting phase of the jelly. As in the case of the pure jelly, the material again deformed under its own weight but now two qualitatively different buckling modes are evident in Fig. 4(b and c). The pattern switch is clear in Fig. 4(b) where the rods are initially aligned in the direction of gravity ('g'). On the other hand, when the sample was rotated through ninety degrees so that the rods were in a direction orthogonal to 'g', the pattern switch was not found and instead shear bands formed under compression as in the example shown in Fig. 4(c). In this

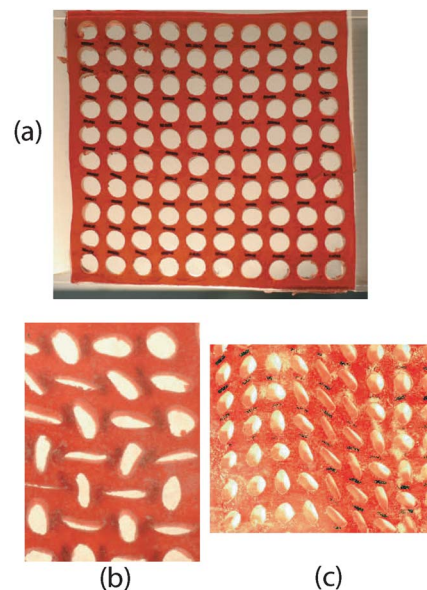


Fig. 4 Jelly samples where additional anisotropy has been introduced into the sample using a set of 8 mm long, 1 mm diameter aluminium (Young's modulus ~ 70 GPa) rods which were placed above each hole during the moulding process. The initial undeformed state where the sample was laid flat and unstrained is shown in (a). (b) A patterned switched state which was formed when the sample was oriented with gravity ('g') parallel with the rods. (c) A shear band forms when the sample is oriented such that 'g' lies in a direction orthogonal to the rods.

case buckling was confined within the layers of rods and was not a global effect but remained localised.

A combination of two materials was used to manufacture the soft cellular solid shown in Fig. 5. It comprised a 10×10 square array of holes in a silicone rubber sheet where the holes were filled with jelly. Filling the holes with a more rigid material than the matrix does not lead to any significant results.⁷ However, when a far weaker material was placed in the holes, a pattern switch was observed above a critical strain of $\epsilon \sim 0.04$ *i.e.* very close to the value found for the case of air holes discussed above. Hence inclusion of a material which has a Young's modulus of $\leq 1\%$ of the bulk does not suppress the pattern switch and has an insignificant effect on the critical strain.

A sample which contained a 5×5 array of circular holes was manufactured using a visco-elastic fluid which is sold as Dittman's therapeutic putty. The material is essentially a stiff variant of the viscoelastic material 'silly putty'. It has a very high viscosity of $\sim 10^5$ Pa s and hence flows slowly over periods of hours. On the other hand it is an elastic solid if strained on short timescales. The sample was produced by refrigerating for ~ 3 hours which aided removal from the mould. The material has a shear modulus of ~ 260 kPa and hence buckled under compression. It was positioned horizontally on the lubricated surface of a compression rig and strained uniaxially at a rate of 1 s^{-1} for 5 mm. It was found that the sample was sufficiently rigid to maintain its original structure for ~ 1 hour if unstrained and pattern switched above a critical strain as shown in Fig. 6.

The results obtained for the square array of circular holes suggests that other periodic elastomeric structures with appropriate symmetry will have similar properties. This is highlighted using the uniaxial compression of a rectangular array of elliptical holes and the results are shown in Fig. 7. In this case compression was applied in a direction perpendicular to the major axis of the constituent elliptical holes. The nominal stress-strain behaviour is shown in Fig. 7. As for circular holes, the relationship is initially linear with homogeneous compression up to a strain of 0.03. At this strain there is a pattern transformation and the stress plateaus. The transformation is a result of a local elastic buckling instability of the vertical ligaments with rotation of interstitial ligatures in opposite directions. The collective behaviour results in a reversible and repeatable pattern transformation to an alternating array of high and low aspect ratio ellipses where the aspect ratio

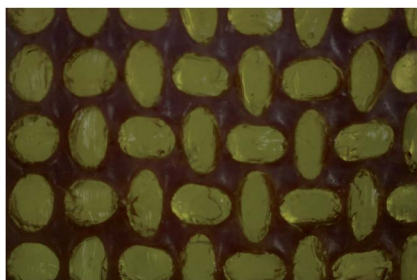


Fig. 5 Silicone rubber sample with jelly filling each of the holes. *N.B.* The jelly adhered to the rubber and retained contact with it throughout the pattern switch.

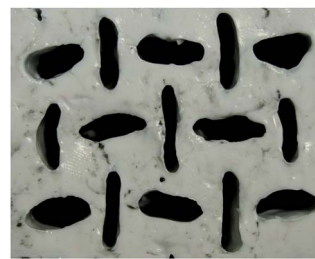


Fig. 6 Pattern switch in the deformation of a visco-elastic fluid. This image (of the central region of the sample) was taken ~ 1 minute after the sample containing a 5×5 square array of circular holes which had been laid on a lubricated flat bed and compressed.

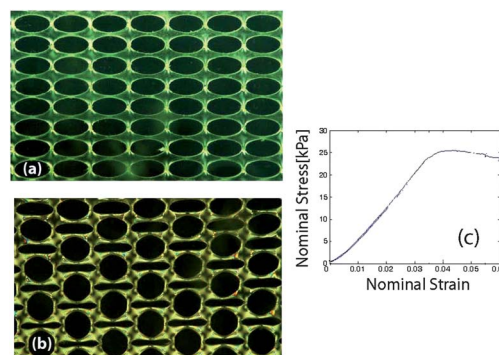


Fig. 7 Uniaxial compression of a rectangular array of ellipses. The sample was 133.2×102.5 mm by 6.9 mm thick, containing a 12×17 rectangular array of elliptical holes of size 5.01 mm (major axis) by 2.67 mm (minor axis) with hole spacing of 5.99 mm vertically and 11.02 mm horizontally. The direction of compression was orthogonal to the minor axes of the ellipses. Compression in the orthogonal direction results in the same pattern at a value of ϵ which is ~ 0.5 smaller than required for the transformation shown here *i.e.* approximately the same as the axis ratio of the ellipses. An experimental stress-strain plot is shown in (c).

contrast increases with increasing macroscopic strain and the low aspect ratio ellipses become nearly circular. The final pattern which emerges is independent of the direction of the applied strain and the ratio of the critical strain required for the pattern transformation is approximately proportional to that of the major to minor axes indicating that it is the stiffness ratio of the repeat unit which sets this global property.

The effect of cell shape was also investigated using 2D cellular structures with square and diamond-shaped voids shown in Fig. 8(a) and (b). The 4×4 square array with 10 mm sided voids with a void fraction of ~ 0.45 were moulded in silicone rubber. The buckled states display qualitatively different features as shown in Fig. 2 although it can be seen that the stress-strain plots are qualitatively similar to each other. The diamond shaped lattice is clearly weaker than the square one as it buckles at ~ 0.75 of the applied strain and supports $\sim 2.5 \times$ smaller stress than the square one. The pattern which develops when the diamond geometry sample was compressed above the critical strain is shown in Fig. 8(d) and a pattern switch was found which is qualitatively similar to the elliptical patterns observed with circular holes. Instead of ellipses, the diamond shaped voids form rhombi which are oriented orthogonally to

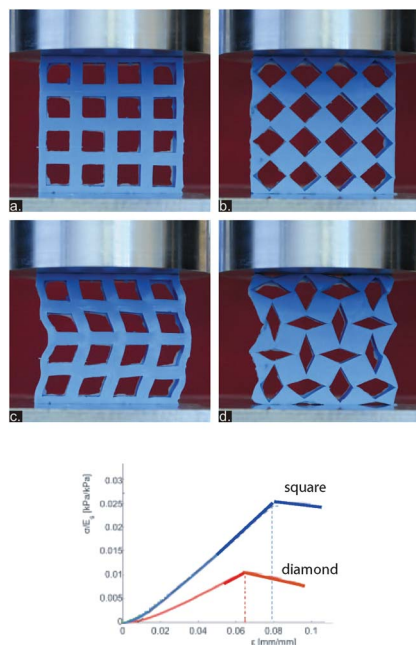


Fig. 8 Images of the compression of an array of square (a and b) and diamond (c and d) holes in a silicone rubber matrix. Both have the voidage fraction of 0.45 and the images were taken at $\epsilon = 0.03$ (a and b) and $\epsilon = 0.1$ (c and d). Experimental stress–strain plots for the respective cases are shown below the images.

their neighbours. This example can be considered as a practical realization of the model problem of rotating tessellated squares which has a Poisson's ratio of -1 .^{11,12} Hence the material shrinks laterally by the same amount it is compressed by. The second example shown in Fig. 8(a) and (c) is a lattice of squares which does not show a pattern switch but simply buckles so that there is localized shearing of the voids. This is perhaps a surprising result since a simple strut model of a square lattice does show coupled buckling¹³ as discussed below.

3 An elemental mechanism

The mechanism which gives rise to the pattern switch can be understood using a simplified model shown in Fig. 9. In this the rubber matrix has been replaced by a skeleton of elastic

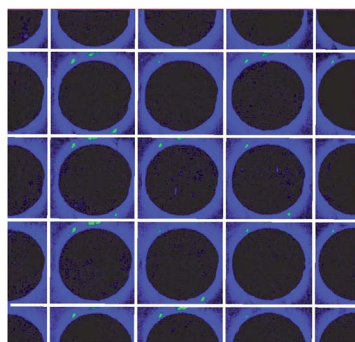


Fig. 9 A schematic diagram illustrating how a skeletal arrangements of Euler struts (shown in white) can be used to represent the full elastomer sample.

classical Euler struts¹⁴ shown in white. The pattern switch which results from the compression of the array is shown in Fig. 10. The initial square array in Fig. 10(a) loses stability above a critical load to a pair of buckled states shown in Fig. 10(b) and (c) when it is compressed uniaxially. In the buckled states it can be seen that elastic 'waves' have travelled across the array from top to bottom and side-to-side and that each of the interstitial points has rotated in alternate directions.

A measure of this bifurcation event was made in experiments on 10×10 arrays of holes in an elastomer. The measure of the bifurcation is the ratio of the vertical to horizontal dimension of the holes which were averaged over the central 36 holes of the 10×10 array. A fixed set of reference holes was used in each case and averaging was performed in pairs. A pitchfork bifurcation is uncovered where a circular array of holes (ratio = 1) is replaced by an array of orthogonal ellipses with increasing (or decreasing) ratios. A simple model for the buckling of a single Euler strut is given by¹⁵

$$\dot{x} = \lambda x - x^3 \quad (1)$$

where λ is the load parameter and x is the deflection of the middle of the beam. $x = 0$ is a solution of the equation for all λ but it can easily be shown that there are two more real stable solutions $x = \pm\sqrt{\lambda}$ for $\lambda > 0$ together with the unstable trivial $x = 0$ state. In the case of the pattern switch the array of coupled

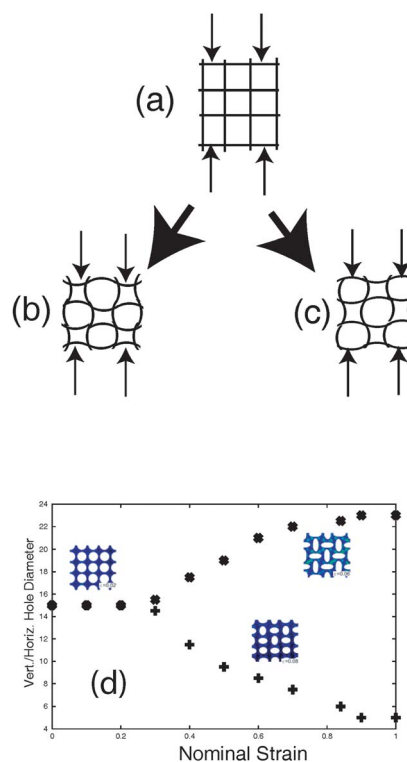


Fig. 10 The compression of the skeletal sample (a) results in buckling of the Euler struts above a critical load to produce two buckled states (b) or (c).¹³ An experimental bifurcation diagram is given in (d) where the measure of the state is the ratio of the vertical to horizontal dimension of the holes averaged over the central 36 holes of 10×10 array of circular holes. The hole dimension ratios were measured w.r.t. the same preselected hole.

Euler struts gives a single global pitchfork bifurcation because of the strong coupling which is present in the square array. An interesting feature which is evident in the experimental bifurcation diagram is that the bifurcation is sharp despite the inevitable presence of imperfections. This is perhaps an indication that the imperfections are in some sense ‘averaged out’ in the square array.

4 Discussion

In conclusion, we have shown that pattern switching is a robust phenomenon when a soft cellular solid containing a square array of circular holes is compressed. The effect does not depend on the details of the properties of the elastic matrix. The robustness is striking and perhaps surprising since only approximately square geometries can be made in practice. Hence the presence of manufacturing imperfections are relatively unimportant. Of greater importance than either the material properties or the presence of imperfections is the symmetry of the lattice and its repeat unit. While square lattices may be weak structures from an engineering perspective, they have important optical properties at the nanoscale and the nonlinear features discussed here persist to very small scales.[†] Hence, these observations at the macroscale open the door for exploring novel metamaterials at a convenient laboratory scale and they in turn provide insights into mechanisms which control properties at the nanoscale.

Acknowledgements

The authors are grateful to Andrew Hazel for many helpful comments on an earlier draft of this paper. Gerd Pfister provided the Dittman’s putty.

References

- 1 L. J. Gibson and M. F. Ashby, *Cellular Solids, Structure and Properties*, Cambridge University Press, 1997.
- 2 P. Vukusic and J. R. Sambles, *Nature*, 2003, **424**, 852–855.
- 3 X. Zhu, G. Wu, R. Dong, C. Chen and S. Yang, *Soft Matter*, 2012, **5**, 2412–2418.
- 4 S. Singamaneni and V. V. Tsukruk, *Soft Matter*, 2010, **6**, 5681–5692.
- 5 T. Mullin, S. Deschanel, K. Bertoldi and M. C. Boyce, *Phys. Rev. Lett.*, 2007, **99**, 084301.
- 6 Y. Zhang, E. A. Matsumoto, A. Peter, P.-C. Lin, R. D. Kamien and S. Yang, *Nano Lett.*, 2008, **8**, 1192–1196.
- 7 J. Michel, O. Lopez-Pamies, P. Ponte Castan and N. Triantafyllidis, *J. Mech. Phys. Solids*, 2007, **55**, 900–938.
- 8 R. Lakes, *Science*, 1978, **235**, 1038–1040.
- 9 K. Bertoldi, P. M. Reis, S. Willshaw and T. Mullin, *Adv. Mater.*, 2010, **22**, 361–366.
- 10 A. Greenhill, *Proc. Cambridge Philos. Soc.*, 1881, **4**, 65.
- 11 D. Attard and J. Grima, *Phys. Status Solidi B*, 2008, **245**, 2395–2404.
- 12 J. Grima, A. Alderson and K. E. Evans, *Phys. Status Solidi B*, 2005, **242**, 561–575.
- 13 N. Ohno, D. Okumura and T. Niikawa, *Int. J. Mech. Sci.*, 2004, **46**, 1697–1713.
- 14 A. Love, *Treatise on the Mathematical Theory of Elasticity*, Dover, 1944.
- 15 S. Strogatz, *Nonlinear Dynamics and Chaos: With Applications to Physics, Biology, Chemistry, and Engineering (Studies in Nonlinearity)*, Perseus, 1994.